AD NUMBER
AD345966
CLASSIFICATION CHANGES
TO: unclassified
FROM: restricted
LIMITATION CHANGES
TO: Approved for public release, distribution unlimited
FROM: Controlling Organization: British Embassy, 3100 Massachusetts Avenue, NW, Washington, DC 20008.
AUTHORITY
DSTL, DSIR 23/29382, 22 Jul 2008; DSTL, DSIR 23/29382, 22 Jul 2008

2

[redacted]

[redacted]

AD345966

BRITISH AIRCRAFT CORPORATION LIMITED

GUIDED WEAPONS DIVISION - BRISTOL

TECHNICAL REPORT NO. 75

A CORRELATION OF FREE FLIGHT AERODYNAMIC HEAT TRANSFER MEASUREMENTS ON POINTED CONES

BACL/GWE/TR/75 JANUARY, 1962.

CONFIDENTIAL RESTRICTED

TECHNICAL REPORT No. 75

COPY No. 120

DATE JANUARY 1962

TITLE

A CORRELATION OF FREE FLIGHT AERODYNAMIC HEAT TRANSFER MEASUREMENTS ON POINTED CONES FOR MACH NUMBERS UP TO 5.0 AND REYNOLDS NUMBERS UP TO 1.7 x 10^8 FOR TURBULENT FLOW

PREPARED ON BEHALF OF BRITISH AIRCRAFT CORPORATION BY

G.W. Aerodynamics Office,
BRISTOL AIRCRAFT LIMITED

AUTHORISATION

Mr. P. D. Rosser, Chief Aerodynamicist (G.W.)

BRITISH AIRCRAFT CORPORATION

THIS REPORT HAS BEEN PRODUCED UNDER M.O.A. CONTRACT KU/20/010/C.B. 31(a).

BRISTOL AIRCRAFT LIMITED

GUIDED WEAPONS ENGINEERING DEPARTMENT

TECHNICAL REPORT No 75

"A CORRELATION OF FREE FLIGHT AERODYNAMIC HEAT TRANSFER MEASUREMENTS ON POINTED CONES FOR MACH NUMBERS UP TO 5.0 AND REYNOLDS NUMBERS UP TO 1.7×10^8 FOR TURBULENT FLOW"

by

M.W.R. SEEL

R. A. BREWER

P.R. BIGNELL

REF. GW/78C/21/AED/1073

DECEMBER, 1961

SUMMARY

Data obtained from free flight tests on pointed cones having semi-angles from 5° to 35° at Mach numbers from 2 to 5 and Reynolds numbers up to 1.7×10^8 are correlated with simple theoretical formulae. A detailed analysis of the errors in the experimental measurements is presented and from correlations of data having an accuracy of ± 10% or better, the following conclusions were made:- (a). For Reynolds numbers greater than 2×10^7 the experimental Stanton numbers exceed the theoretical conical values by about 11%. (b). The effect of cone-angle on the correction factor applied to flat plate theory to adjust it to conical flow conditions appears to be quite random, the data falling around the normally recommended value of 1.15. (c). The skin temperature, at least for fully turbulent conditions, can be predicted to a high order of accuracy by Hill's method in conjunction with Van Driest's theory. (d). Reynolds analogy is well verified by the data and is found to be independent of both Mach number and Reynolds number effects. (e). Owing to poor presentation of the wall temperature data in most of the reports the recovery factor data was found to be unreliable.

The following recommendations, based on the results of this investigation, may be made with regard to any future free flight tests on pointed cones:-

1) Owing to the paucity of data for Reynolds numbers higher than 2×10^7, tests could profitably be designed to investigate this region.

2) Some tests in the cone-semi angle range from 15° to 30° either in free flight or wind tunnels would be of value in finally assessing whether or not the correction factor, mentioned above, is a function of cone semi-angle.

3) Every effort should be made to locate the transition point during flight if reliable comparisons are to be made between theory and experiment for turbulent flow.

DISTRIBUTION LIST

DISTRIBUTION	COPY NO.
Mr. R. A. Shaw M.O.A.	1 - 10
Mr. R. J. Monaghan Defence Research Staff, British Embassy, Washington 8, D.C.	11 - 40
Mr. D. Evans (For O.N.E.R.A.) Scientific Attache, British Embassy, 35, Rue Du Fg. St. Honore, Paris 8e.	41 - 70
Mr. R. W. Gandy A.R.C.	71 - 100
R.A.E. Farnborough	
Dr. L. F. Crabtree	101
Mr. J. Hamilton	102
Aero Library	103
G.W. Library	104
R.A.E. Bedford	
Library	105
British Aircraft Corporation:	
English Electric (Luton)	
Mr. A. C. Southgate	106
Vickers Aircraft Limited (Weybridge)	
Mr. M. W. Salisbury	107
Bristol Aircraft Limited	
Mr. D. J. Farrar	108
Mr. P. D. Rosser	109
Aero 'N' File	110
Central Records	111
G.W. T.I.B.	112
A.E.O. Library	113
Spares	114 - 120

1. Introduction.

A number of reports presenting the results of free flight tests to determine the aerodynamic heating characteristics of pointed cones have been published in recent years. Generally, these tests were made for specific cone semi-angles and trajectories. The present report correlates the available free flight data for all the available test results and compares it with the existing theories on aerodynamic heat transfer to pointed cones.

Simple 'incompressible' and 'compressible' correlations of all the data are first presented and, after a detail assessment of the probable errors in the experimental measurements, points having an accuracy of ± 10% or less, are retained in the rest of the analysis. In particular, the analysis has been aimed at investigating the following topics:-

a) Prediction of heat-transfer rates (i.e. Stanton numbers) and wall temperatures.

b) Finding evidence in support of Reynold's analogy.

c) Temperature recovery factor values.

d) The effect of cone semi-angle on the heat transfer rate.

Owing to the small quantity of laminar flow data presented it was decided to carry out an investigation of the turbulent flow data only.

Section 2 gives details of the methods used to reduce and present the data, and Section 3 presents a discussion of the results. The final conclusions of the investigation are noted in Section 4.

2. Data reduction and presentation of results.

2.1. Data Reduction Programme

Experimental data from free flight tests is normally presented in the non-dimensional form of local Stanton number or as a dimensioned heat flux. A data reduction programme was written to reduce all the data to a common form for the purposes of correlation. Variable specific heat calculations were made throughout and the Eckert reference temperature was deduced from the reference enthalpy given below (in the usual way).

$$i^* = i_1 + 0.5\,(i_1 - i_w) + 0.22\,(i_r - i_w)$$

$$\text{with } i_r = i_1\left(1 + \frac{\gamma - 1}{2} M_1^2\right)$$

and r = 0.89 (Turbulent flow conditions only have been considered).

N.B. All Symbols are given in Appendix I.

2.2. Presentation of Results.

(a) 'Incompressible' correlation (Nu_x; Re_x)

Fig. 1 shows the correlation of data from five free flight tests in the 'incompressible' form of Nu_x vs Re_x. The theoretical curves for incompressible flow derived in Appendix II are also shown on Fig. 1.

(b) Fig. 2 shows the results from six free flight tests correlated on an "intermediate flow conditions" basis in the form $S_t^* (Pr^*)^{2/3}$ vs. Re^*. The corresponding theoretical curves derived in Appendix II are also shown.

(c) Estimation of probable errors in the measured Stanton numbers.

It is shown in Appendix III that the errors in S_t^* are related to those in S_t as follows:-

$$\frac{\sigma S_t^*}{S_t^*} \simeq \left(\frac{\sigma S_t}{S_t}\right)$$

The function $\sigma S_t/S_t$ derived from equation (3) of Appendix II, is shown in Fig. 3 for the flight data of Ref. 5. The values of $\sigma S_t/S_t$ were evaluated, as functions of the flight time, at one station on each of the cones analysed.

The results for the chosen station were then assumed to apply to the other measuring stations. In Fig. 4, the results with less than 10% error in S_t^* are presented in the same form as Fig. 2. (The error in P_r^* is negligible). The vertical lines attached to each point on the plot indicate the probable range in which the parameter $S_t^* (Pr^*)^{2/3}$ lies. The points for which the estimated probable errors in S_t^* do not exceed 10% are retained throughout the rest of the results presented. The transitional points shown on Fig. 2 are also dropped from Fig. 4 and later plots.

The estimated errors in Re^* (See Appendix III) are such that they will not influence significantly the correlation presented in Fig. 4.

(d) Effect of basing Re^* on distance measured from transition point.

Of the reports analysed only Ref. 5 presented data for the location of transition along the cone surface. For this data it was therefore possible to introduce a modified Reynolds number defined as:-

$$R_e^* (x-x_T) = \frac{\rho^* U_1}{\mu^*} (x - x_T)$$

as a basis for correlating the heat transfer measurements in turbulent flow. Fig. 5 shows the variation of $S_t^* (P_r^*)^{2/3}$ with $R_e^* (x-x_T)$

(e) <u>The effect of cone angle on the ratio of conical to flat plate values of the heat-transfer coefficient.</u>

A correction factor relating conical flow conditions to those on a flat plate may be expressed in the form

$$\xi = \frac{S_t^* (P_r^*)^{2/3}\ \text{cone}}{S_t^* (P_r^*)^{2/3}\ \text{flat plate}}$$

By finding the values of $S_t^* \ (P_r^*)^{2/3}_{\text{cone}}$ compared with the flat-plate value of this parameter for the same local flow conditions for one cone angle, the experimental value of ξ was evaluated from

$$\xi = \frac{1}{n} \sum_{m=1}^{n} \frac{(S_t^* \cdot (P_r^*)^{2/3}_{\text{cone, exp.}})_m}{S_t^* \cdot (P_r^*)^{2/3}_{\text{Plate}}} \qquad (1)$$

(where n = no. of experimental points).

The arithmetic mean was used since the number of points available for evaluating ξ for each flight were insufficient to justify finding standard deviations by the root mean square method.

Van Driest in Ref 12, has suggested that ξ should be a constant independent of Mach number, Reynolds number and cone angle (providing this is not too large). The value of ξ suggested is

$$\xi = (2)^{1/5} \doteq 1.15.$$

The values of ξ derived from the results for six flights using equation (1) are shown in Fig. 6 together with the theoretical line $\xi = 1.15$ as a function of the cone semi-angle θ.

(f) <u>Correlation of the parameter $\left\{\frac{S_t \ \text{exp}}{S_{t_i}}\right\}$ with the intermediate temperature ratio T^*/T_1.</u>

In Appendix II part 2, it is shown that the ratio of compressible to incompressible Stanton numbers depends essentially upon the ratio T^*/T_1. The relation derived in Appendix II is:-

$$\frac{(S_t)_{\text{exp.}}}{S_{t_i}} = \left\{\frac{T^*}{T_1}\right\}^{-0.66}$$

The theoretical values of S_{t_i} were derived from the Prandtl-Schlichting incompressible skin friction coefficient formula (Equation (7) of Appendix II) and modified to conical flow conditions using the factor 1.15. The correlation of the ratio (S_t) exp/S_{t_i} with (T^*/T_1) is shown in Fig. 7 together with a plot of the theoretical curve given by the equation quoted above.

(g) **Correlation of the experimental results in the form $(St)_{exp}/(St)_i$ against local Mach number and wall temperature ratio Tw/T_1.**

In order to obtain the dependence of Stanton number on Mach number the results derived from five free-flight tests are plotted seperately in Figs. 8 (a) to (e) in the form,

$$\frac{(St)_{exp}}{(St)_i} \quad \text{vs} \quad M_1$$

(where St_i was found by the method described in the previous Section) Inspection of equations (6), (8) and (9) in Appendix II show that such a correlation is strongly dependent upon the values of Tw/T_1 and, to a much lesser extent, upon the value of the local Reynolds number Re_1. Owing to the inevitable small variations in Tw/T_1 for each experimental point, the results are presented in ranges of Tw/T_1, each range having a separate symbol as shown in the figures.

The theoretical curves were derived from equations (4) and (8) of Appendix II and are presented for the maximum and minimum values of Tw/T_1 encountered during flight and are based on the mean Reynolds number during the time measurements were made.

(h) **Reynolds Analogy Factor**

As shown in Appendix II part 3, it is possible to obtain estimates of Reynolds analogy factor from experimental measurements of Stanton number. Figs 9 and 10 show the values of Reynolds analogy factor found from six free flight tests as functions of Re and local Mach number respectively. On both these plots the value $S = P_r^{2/3}$ suggested by Colburn (Ref 13) are shown for the purpose of comparison.

(i) **Recovery Factor Data.**

As explained in Appendix II part 4, it was not possible to obtain reliable estimates of the turbulent temperature recovery factor from the flight tests presented in Refs 2, 3 & 6. However, in seeking for trends of the recovery factor with local Mach number and Reynolds number these results are presented in Figs 11 and 12 respectively. Ref. 7 also presents results for recovery factor measurements on the NACA RM-10 missile and these are more reliable than those just mentioned. These have also been presented on Figs. 11 and 12. Various theoretical values are also shown on Fig. 11 and extrapolated data from Ref. 9 on continuous flow tunnels is shown for comparison on Fig. 12.

(j) **Wall temperature measurements**

In order to assess Hill's method (Ref. 10) for predicting the wall temperature of thermally thin skins during flight, two specimen calculations of wall temperature variation based on Hill's method were made for two extreme values of the cone semi-angle. Hill's equation is presented in Appendix II part 5, and the value of G was found for an average value of the wall temperature over the time range investigated. The heat transfer coefficients were evaluated from Van Driest's theory (Ref. 11). The results for a typical fully turbulent station on the cone tests reported in Refs. 2 and 6 are shown in Figs 13 and 14 respectively. The radiation terms were not included in these calculations.

3. Discussion.

3.1. Nusselt Number and Stanton Number Correlations.

Correlations on a Nusselt or Stanton number vs. Reynolds number basis are shown in Figs. 1, 2, 4 and 5. The results shown on Fig. 1, which are on a local flow conditions basis, show that the trend of the experimental results follows that predicted by incompressible flow theory.

If the results are corrected for compressibility effects using the Eckert reference temperature correction method, they can be re-plotted in the form $St^{*}(Pr^{*})^{2/3}$ vs. Re^{*}. This plot is shown in Fig. 2 and it will be seen, by comparison with Fig. 1, that the experimental points are in much better agreement with the theoretical curves. The results from Ref. 3 for 'intermediate' Reynolds numbers greater than about 2×10^{7} lie well above the theoretical predictions. However, since these results are derived from one particular flight a modification of the theory in this region is not justifiable.

The results shown on Fig. 4. include all the points shown on Fig. 2. for which the error in St^{*} is estimated to be less than about 10%. (See section 2.2.c. and Appendix III). Within this band of accuracy the results (excluding those from Ref. 3) show no definite bias towards either theoretical curve presented. Even considering the points with the smallest errors the distribution about the two theoretical lines remains fairly random. The results shown for Re^{*} greater than about 2×10^{7} still lie well above either theoretical line. Despite the fairly good accuracy of these points as estimated on the assumptions described in Appendix III, it is quite possible that they may be in error due to an error peculiar to that flight which is not accounted for in the general error analysis presented in this report.

Considering the results shown in Figs. 1, 2 and 4, it may be concluded that, the recommended curve for turbulent heat-transfer to pointed cones will give a reliable estimate of heat-transfer to pointed cones at least up to local Reynolds numbers of 5×10^{7}. To confirm the recommended curve for local Reynolds numbers greater than 5×10^{7} would require more experimental evidence than that currently available from free flight tests.

As previously described in Section 2.2.d, it was only possible to investigate the influence of transition on the correlations for the results of Ref. 5. Comparing the results shown with the corresponding ones on Fig. 4, the correlation is not significantly improved by the modification of Re^* described in section 2.2.d. Points such as those for Ref. 3. previously discussed, however, could well fall on the theoretical curves when correlated on the basis of Fig. 5. It may be concluded from this that, if reliable deductions are to be made from free flight measurements of aerodynamic heating phenomena, more effort should be put into providing a means of locating the transition point during flight than appears to have been put into this problem to date.

3.2. The effect of cone angle on the correction factor applied to flat plate theory to estimate conical flow values of the Stanton number.

Fig. 6 shows the variation of the correction factor ξ, defined in section 2.2.e., with cone semi-angle θ. Owing to the random distribution of the experimental values of $St^* (Pr^*)^{2/3}$ about the theoretical lines discussed in the preceeding section and also to the relatively few cone angles investigated, no definite trend of ξ with θ is found. This result points to the need for free flight tests to be carried out for a wider range of cone angles than those hitherto tested.

3.3. Correlation of the parameter (St) exp./St_i with the intermediate temperature ratio and Mach number.

Fig. 7 shows a correlation of the experimental results in the form of (St) exp/$(St)_i$ against T^*/T_1. Within the error bands previously selected for the analysis (Section 2.2.c), the results agree with the simple theoretical law derived in Appendix II part 2. With the results correlated in this manner, it can be seen that, on average the simple theory for conical flow conditions generally overestimates local Stanton number and hence, overestimates the local heat-transfer coefficient.

Figs 8 (a) to (e) are an attempt to show the effect of local Mach number on the value of Stanton number. Owing to the fact that the values of Tw/T_1 in flight generally increase with Mach number it is almost impossible to present experimental data for constant values of Tw/T_1 as a function of local Mach number. The plots show that the data is in fair agreement with the theoretical predictions of Mach number effects.

3.4. Reynolds Analogy factor and recovery factors.

Fig. 9 shows the variation of Reynolds analogy factor with Reynolds number based on intermediate temperature conditions and Fig. 10 shows the same factor as a function of Mach number. The theoretical value of Reynolds analogy factor based on a Prandtl number of 0.72 represents a good mean through the data. In addition to this, it may be concluded that Reynolds analogy factor for pointed cones is independent of both Mach number and Reynolds number for the range of these parameters investigated.

Nothing may be concluded from the part of the investigation dealing with the recovery factors. The estimated recovery factors are shown as functions of the local Mach number and Reynolds number in Figs. 11 and 12 respectively. Crudely, the data in Fig. 11 shows a tendency for the recovery factor to decrease with increasing local Mach number, as predicted by Tucker and Maslen (Ref.8), but is by no means conclusive. The reasons for these poor results for the recovery factor are detailed in Appendix II part 4. Fig. 12 does not show any distinct evidence that the recovery factor decreases with increasing Reynolds number as observed by Monaghan in Ref (9) from a survey of continuous flow tunnel measurements.

3.5. Estimation of wall temperatures.

A comparison of the theoretical and experimental variation of wall temperature with time for two typical flights is shown in Figs. 13 and 14. The results shown for the 5° semi-angle cone on Fig. 13. show excellent agreement with the theoretical prediction based on Hill's method (Ref. 10) using Van Driest's theory for predicting the heat-transfer coefficients (Ref. 11).

The results for the 35° semi-angle cone, however, are not quite as good, there being a discrepancy of 9% between the predicted and measured maximum temperatures. The theoretical prediction can, of course, be improved by making allowance for radiation effects which were not included in the present calculation.

Bearing in mind, from the results shown in Fig. 4, that the theoretical Stanton numbers for these flights differ from the experimental Stanton numbers by the order of 10%, Hill's method can be said to give an excellent prediction of the wall temperature for thin skins.

4. Conclusions.

1) Some attempt should be made to obtain free flight heat-transfer measurements at Reynolds numbers greater than 10^7, where the available results appear to be unreliable.

2) Owing to the low Mach number range covered by the free flight data available, it is proposed to extend the present correlation to higher Mach numbers using wind tunnel results.

3) Where possible, every effort should be made to obtain evidence of transition location during flight so that reliable estimates of the effective Reynolds number in turbulent flow can be made.

4) No influence of cone angle on the magnitude of the Stanton number compared with the equivalent flat plate Stanton number could be established from the results. This was primarily due to the small range of cone angles investigated in free flight. If more free flight tests are done it would be worth investigating cone semi-angles in the range 15° to 30°.

5) The trends of the experimental results follow the theoretical predictions in the main, except for the results available at Reynolds numbers greater than 2 x 10^7.

6) Reynolds analogy factor was found to be independent of both Mach number and Reynolds number as predicted by simple theory.

7) Recovery factor data deduced from the presented experimental results are, in general, unsatisfactory. This is primarily due to the small scales used for presenting wall temperature - time plots in the reports and the lack of tabulated values of the actual measured wall temperatures.

8) Hills method for predicting the temperature of thermally thin skins, when used in conjunction with Van Driest's theory for predicting the heat-transfer coefficients, give reliable estimates of the wall temperature.

REFERENCES

1.	L. RABB S.H. SIMPKINSON.	Free flight measurements on two 20° cone-cylinders at Mach numbers from 1.3 to 4.9. NACA RM E55F27 (JULY 1955)
2.	C.B. RUMSEY R.C. PILAND R.N. HOPKO	Aerodynamic heating data obtained from free flight tests between Mach numbers of 1 and 5. NASA TN D-216 (JANUARY 1960)
3.	C.F. MERLET C.B. RUMSEY	Supersonic free flight measurement of heat transfer and transition on a 10° cone having a low temperature ratio. NACA RM L56L10 (JANUARY 1957)
4.	C.B. RUMSEY D.B. LEE	Measurements of aerodynamic heat transfer and boundary layer transition on a 15° cone in free flight and Mach numbers up to 5.2 NACA RM L56F26 (OCTOBER 1956)
5.	C.B. RUMSEY D.B. LEE	Measurements of aerodynamic heat transfer and boundary layer transition on a 10° cone in free flight at Mach numbers up to 5.9 NACA RM L56B07 (APRIL 1956)
6.	R.L. DOMMETT D.I. DAWTON	C.T.V.5. Series 2. Trajectory and heat transfer data from seven firings. RAE. TN GW 515 (MAY 1959)
7.	R.O. PILAND K.A. COLLIE W.E. STONEY	Turbulent and laminar heat transfer measurements on a 1/6 scale NACA RM-10 missile in free flight to a Mach number of 4.2. NACA RM L56C05 (JULY 1956)
8.	M. TUCKER S.H. MASLEN	Turbulent boundary layer temperature recovery factors in two dimensional supersonic flow. NACA TN 2296 (FEBRUARY 1951)
9.	R.J. MONAGHAN	A survey and correlation of data on heat transfer by forced convection at supersonic speeds. RAE TN AERO 2259 (SEPTEMBER 1953).

10. P.R. HILL — A method of computing the transient temperature of thick walls from arbitrary variation of adiabatic wall temperature and heat transfer coefficient.
NACA TN 4105

11. E.R. VAN DRIEST — The problem of aerodynamic heating.
Aero Engineering Review.
(OCTOBER 1956)

12. E.R. VAN DRIEST — Turbulent boundary layer in compressible fluids.
J. AERO SCI. VOLUME 18
(1951).

13. A.P. COLBURN — A method of correlating forced convection heat transfer data and a comparison with fluid friction.
TRANS. AMER. INST. CHEM. ENG. VOL.29
1933

14. H. SCHLICHTING — Boundary layer theory.
PERGAMON PRESS LTD.
(1955)

Appendix 1

List of Symbols

a	Speed of sound	ft/sec.
c	Specific heat of skin material	C.H.U/lb °K.
C_f	Local skin friction coefficient	
C_p	Specific heat at constant pressure	C.H.U./lb °K.
	also, pressure coefficient $\dfrac{p - p_\infty}{\frac{1}{2}\gamma M_\infty^2 p_\infty}$	
G	Thermal capacity of thin skins, (ρcl),	CHU/ft²-°K.
h	Local convective heat transfer coefficient $= \dfrac{q}{(T_r - T_w)}$	CHU/ft²/sec/°K
i	Local static enthalpy	CHU/lb
k	Thermal conductivity	CHU/ft/sec/°K
l	Skin thickness	ft
M	Mach number	
N_u	Nusselt number ($h\,x/k$).	
p	Pressure	lb/ft²
P_r	Prandtl number	($\mu C_p/k$)
q	Heat flux	CHU/ft²/sec.
Re	Reynolds number	($\rho ux/\mu$)
r	Temperature recovery factor.	
S	Reynolds analogy factor	($\frac{C_f}{2} / S_t$)
S_t	Stanton number	($h/\rho UC_p$)
T	Temperature	°K
t	Time	sec.
U	Velocity	ft/sec.
x	Distance along cone surface measured from tip.	ft

γ	Ratio of specific heats	
e	Emissivity	
θ	Cone semi-angle	Degrees
μ	Viscosity	lb/ft-sec.
ρ	Density	lb/ft^3
σ	Deviation in a parameter; also Stefan Boltzmann constant.	$CHU/ft^2/sec/^{\circ}K^4$

Subscripts

1	Local conditions at boundary layer edge.
∞	Free stream conditions.
i	Incompressible flow.
r	Recovery conditions.
s	Stagnation conditions.
T	Transition
W	Wall conditions.

Superscript

*	Evaluated from the Eckert reference enthalpy.

Appendix II

Summary of theoretical equations

1. **Expressions relating Stanton number and Nusselt number to Reynolds number and Prandtl number for turbulent flow on a flat plate.**

The simplest relation between C_f and R_e is given by the equation

$$C_{f_t} = 0.0592\ R_e^{-1/5} \qquad \text{(Ref. 14)} \qquad (1)$$

and, using the modified Reynolds Analogy due to Colburn

$$S_{t_t} = P_r^{-2/3} \left(\frac{C_f}{2}\right)$$

we obtain for the Stanton number in incompressible flow,

$$S_{t_i} = 0.0296\ P_r^{-2/3}\ Re^{-1/5} \qquad (2)$$

Further, we note that N_u is given by

$$N_u = P_r .\ R_e .\ S_t$$

and substituting this expression into equation (2) yields,

$$N_{u_t} = 0.0296\ P_r^{+1/3}\ Re^{+4/5} \qquad (3)$$

The Stanton number in compressible flow is found from equation (2) using the 'intermediate' temperature technique due to Eckert noting that,

$$S_t = S_t^* \left\{\frac{\rho^*}{\rho}\right\} = S_t^* . \frac{T}{T^*} \qquad (4)$$

where, $S_t^* = 0.0296\ (P_r^*)^{-2/3}\ (R_e^*)^{-1/5}$ (5)

and the properties are evaluated at a temperature T^* corresponding to an enthalpy i^* given by

$$i^* = i_1 + 0.5\ (i_w - i_1) + 0.22\ (i_r - i_1) \qquad (6)$$

An alternative expression for the incompressible local skin friction coefficient is the Prandtl-Schlichting formula (Ref.14).

$$C_{f_t} = 0.288\ (\log_{10} R_e)^{-2.45} \qquad (7)$$

and, corresponding to this there can be obtained the following relations;

$$S_{t_i} P_r^{2/3} = 0.144 (\log_{10} R_e)^{-2.45} \qquad (8)$$

and

$$(S_{t_i})_{comp.} = 0.144 \frac{\rho^*}{\rho} (P_r^*)^{-2/3} (\log_{10} R_e^*)^{-2.45} \qquad (9)$$

Equations (3), (5), (8), and (9) can be applied to conical flow by multiplying the right hand side by tho factor 1.15.

2. A Simplified Relation between S_t and S_{t_i}.

Using eqns. (1), (4) and Reynolds analogy, we may write,

$$S_t = 0.0296 (R_e^*)^{-1/5} (P_r^*)^{-2/3} \left\{\frac{T_1}{T^*}\right\} \qquad (10)$$

and, from equation (2)

$$S_{t_i} = 0.0296 R_e^{-1/5} (P_r)^{-2/3} \qquad (11)$$

Hence,

$$\frac{S_t}{S_{t_i}} = \left\{\frac{R_e}{Re^*}\right\}^{1/5} \left\{\frac{T_1}{T^*}\right\} \left\{\frac{P_r}{P_r^*}\right\}^{2/3} \qquad (12)$$

and, assuming (a) $P_r \simeq P_r^*$

(b) $\mu \propto T^{0.7}$

equation (12) reduces to

$$\frac{S_t}{S_{t_i}} = \left\{\frac{T^*}{T_1}\right\}^{-0.66} \qquad (13)$$

where T^* is found from equation (6)

3. Reynolds analogy factor.

Reynolds analogy may be written,

$$\frac{1}{S} = \frac{S_t}{(C_f/2)} \qquad (14)$$

and, $C_{f/2}$ in compressible flow using the Prandtl-Schlichting equation (eqn.7), is

$$\left\{\frac{C_f}{2}\right\}_{Plate} = 0.144 \left\{\frac{\rho^*}{\rho}\right\} (\log_{10} R_e^*)^{-2.45}$$

$$\therefore \left\{\frac{C_f}{2}\right\}_{cone} = 1.15 \left\{\frac{C_f}{2}\right\}_{plate.} \qquad (15)$$

Thus, combining equations (15) and (14), S is found from the experimentally measured Stanton number as follows,

$$S = \frac{6.039\,(S_T)\ \exp.\left\{\frac{\rho}{\rho^*}\right\}}{(\log_{10} R_e^*)^{-2.45}} \qquad (16)$$

(4) Approximate determination of the recovery factors.

The heat balance for an element of the skin neglecting conduction along the skin and internal radiation is,

$$G\,\frac{dTw}{dt} = h\,(T_r - T_w) + \varepsilon_w\,\sigma\,T_w^4 \qquad (17)$$

and, for zero convective heat transfer this becomes

$$G\,\frac{dTw}{dt} = \varepsilon_w\,\sigma\,T_w^4 \qquad (18)$$

In the reports analysed the wall temperatures are presented graphically as functions of time on so small a scale that it was impossible to solve equation (18) by the normal graphical procedure. However, the radiation term in equation (17) was small for most cases and the approximation was made that zero convective heat-transfer conditions obtained at a time when,

$$G\,\frac{dTw}{dt} = 0 \qquad (19)$$

The wall temperature at this time is equal to the recovery temperature, T_r, and the recovery factor is evaluated from the relation

$$r = \frac{T_r - T_1}{T_s - T_1} \qquad (20)$$

(5) Hill's method for predicting skin temperatures on thermally thin skins.

Hill showed in Ref 10, that the wall temperature variation with time (neglecting radiation) could be found from the following equation,

$$(Tw)m = \frac{h_m.\ T_{rm} + (hT_r - hT_W + 2/\delta\ \ GT_W)_{m-1}}{(2/\delta)\ G_m + h_m}$$

where m and m-1 refer to two successive times and δ is the time interval for the calculation.

APPENDIX 3

ERROR ANALYSIS

1 ESTIMATION OF PROBABLE ERRORS IN MEASURED STANTON NUMBER, ST

Following the procedure for estimating errors in ST described in Ref. 7, we define,

$$\left(\frac{\sigma_\phi}{\phi}\right)_{\psi_n} = \left| \frac{\partial\phi}{\partial\psi_n} \cdot \frac{\sigma_{\psi_n}}{\phi} \right| \quad \text{———} (1)$$

where σ_ϕ is the error in ϕ due to errors,

σ_{ψ_n} in the quantities ψ_n.

The total error in ϕ due to errors in j quantities ψ_n is then

$$\left(\frac{\sigma_\phi}{\phi}\right)_{TOTAL} = \left\{ \sum_{n=1}^{j} \left[\left(\frac{\sigma_\phi}{\phi}\right)_{\psi_n}\right]^2 \right\}^{\frac{1}{2}} \quad \text{———} (2)$$

By considering the probable errors in the individual measured or derived quantities, tabulated, the probable error in Stanton number can be shown to be,

$$\left(\frac{\sigma_{ST}}{ST}\right)_{TOTAL} \triangleq \left[\frac{401 + 0.16M_\infty^2 + \{T_1(1-r)0.01\}^2}{(T_r - T_w)^2} + \left(\frac{1}{dT_w/dt}\right)^2 + 0.00132\right]^{\frac{1}{2}}$$

$$\text{———} (3)$$

(N.B. T in $^{\circ}$R in above equation).

Table of probable errors (After Ref. 7).

Quantity	Error
T_w	20°R
T shield	20°R
ρ_∞	0.013 ρ_∞
T_∞	1°R
U_∞	4 ft/sec
dT_w/dt	1°R/sec
ℓ	0.03 ℓ
ρ_1/ρ_∞, T_1/T_∞, U/U_∞	0
ε_w	0.02

2 PROBABLE ERRORS IN ST*, Pr* AND Re* WHICH OCCUR IN THE CORRELATIONS

(a) Error in ST*

$$ST^* = (ST)\left(\frac{\rho_1}{\rho^*}\right) \qquad (4)$$

Hence, using equation (1),

$$\left(\frac{\sigma_{ST^*}}{ST^*}\right)_{ST} = \left|\frac{\partial ST^*}{\partial ST}\cdot\frac{\sigma_{ST}}{ST^*}\right| = \left(\frac{\rho_1}{\rho^*}\right)\frac{\sigma_{ST}}{ST^*} = \frac{\sigma_{ST}}{ST} \qquad (5)$$

and, similarly,

$$\left(\frac{\sigma_{ST^*}}{ST^*}\right)_{\left(\frac{\rho_1}{\rho^*}\right)} = \frac{\sigma_{(\rho_1/\rho^*)}}{(\rho_1/\rho^*)} \qquad (6)$$

Then, using equation (2),

$$\left(\frac{\sigma_{ST^*}}{ST^*}\right)_{TOTAL} = \left\{\left(\frac{\sigma_{ST}}{ST}\right)^2 + \left[\frac{\sigma_{(\rho_1/\rho^*)}}{(\rho_1/\rho^*)}\right]^2\right\}^{\frac{1}{2}} \qquad (7)$$

Now, for the conditions covered by the investigation it can be shown that

$$\frac{\sigma_{(\rho_1/\rho^*)}}{\rho_1/\rho^*} \ll \frac{\sigma_{ST}}{ST}$$

Hence, equation (7) becomes

$$\left(\frac{\sigma_{ST^*}}{ST^*}\right)_{TOTAL} \simeq \left(\frac{\sigma_{ST}}{ST}\right)_{TOTAL} \qquad (8)$$

(b) Error in Pr*

It is readily shown that errors in Pr* will lie in the range ±0.0005. Hence,

$$\frac{\sigma_{Pr^*}}{Pr^*} \simeq 0 .$$

(c) Error in Re*

By using equations (1) and (2) it can be shown that errors in Re* due to errors in T*, ρ_∞, U_∞ and T_∞ will be

$$\frac{\sigma_{Re^*}}{Re^*} \not> 4\% .$$

FIG. 1.

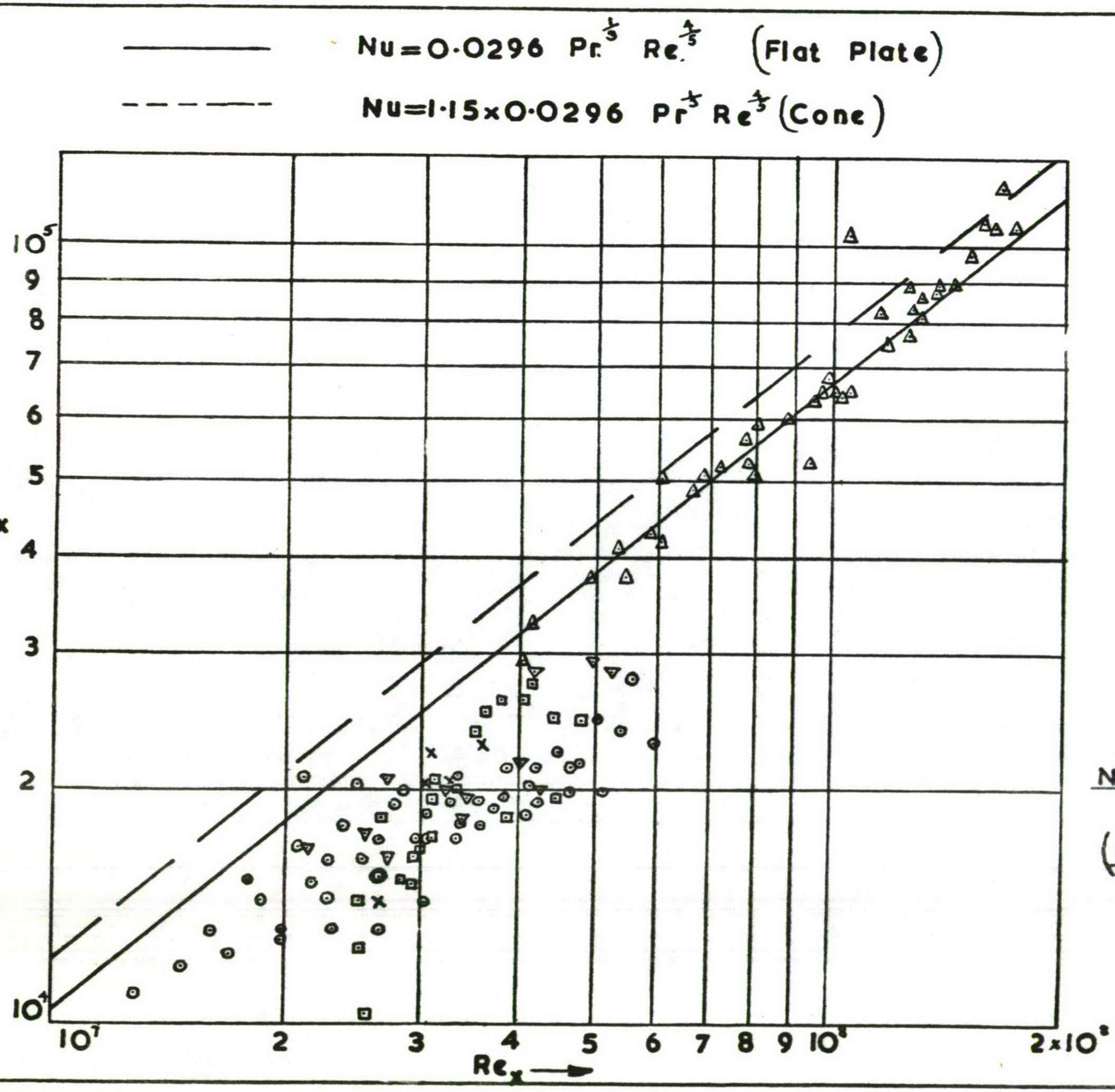

KEY

REF.	symbol	½ angle θ
1	⊙	10°
2	×	5°
3	△	5°
4	⊡	7·5°
5	▽	5°

FIG.I. VARIATION OF LOCAL NUSSELT NUMBER WITH LOCAL REYNOLDS NUMBER (WITHOUT COMPRESSIBILITY CORRECTIONS).

(W.1167).

FIG.2.

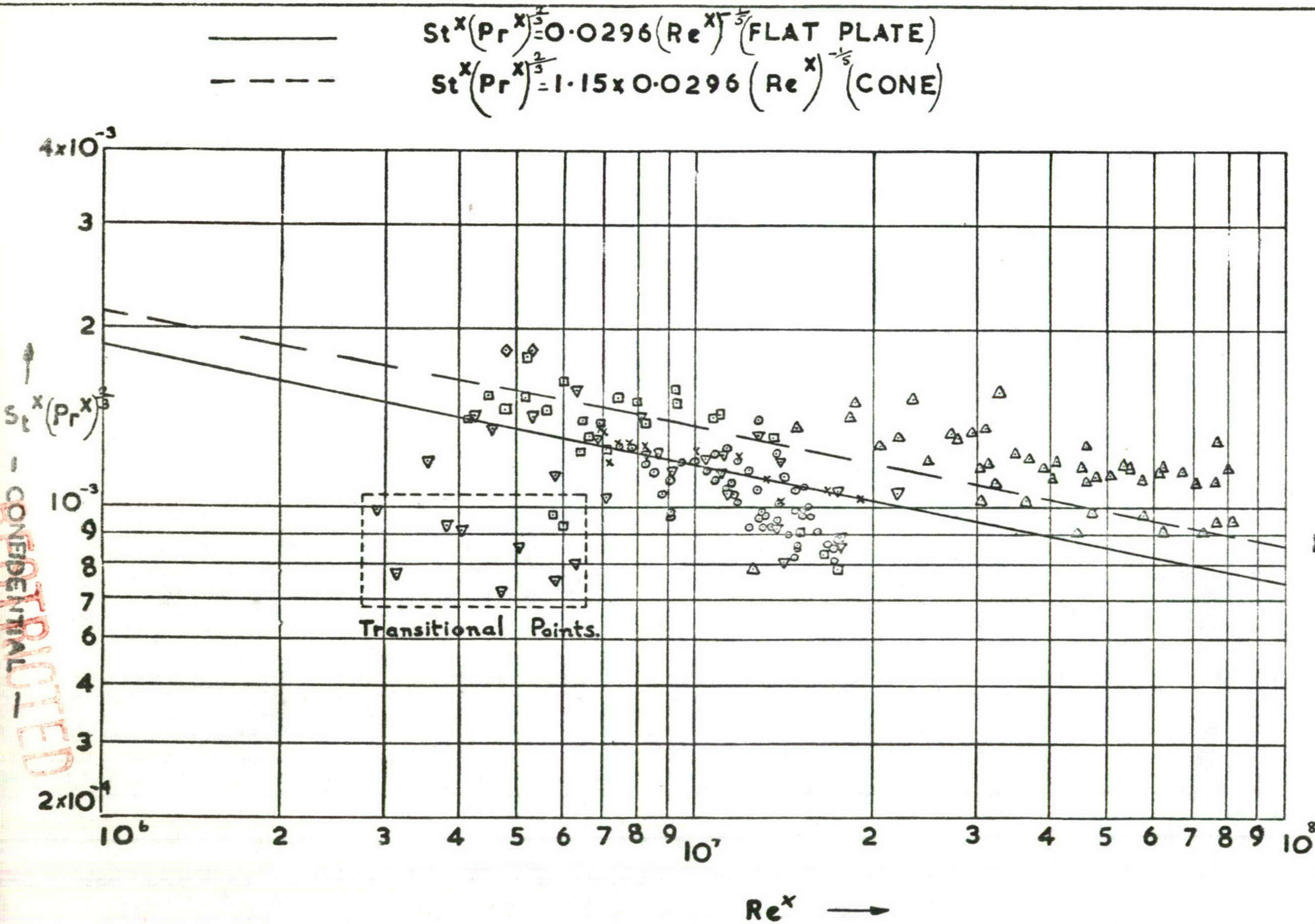

KEY

REF.	symbol	½-angle θ
1	⊙	10°
2	×	5°
3	△	5°
4	⊡	7·5°
5	▽	5°
6	◇	35°

FIG. 2. VARIATION OF $St^x(Pr^x)^{\frac{2}{3}}$ WITH Re^x (CONDITIONS BASED ON INTERMEDIATE TEMPERATURE, T^x)

(P.1167).

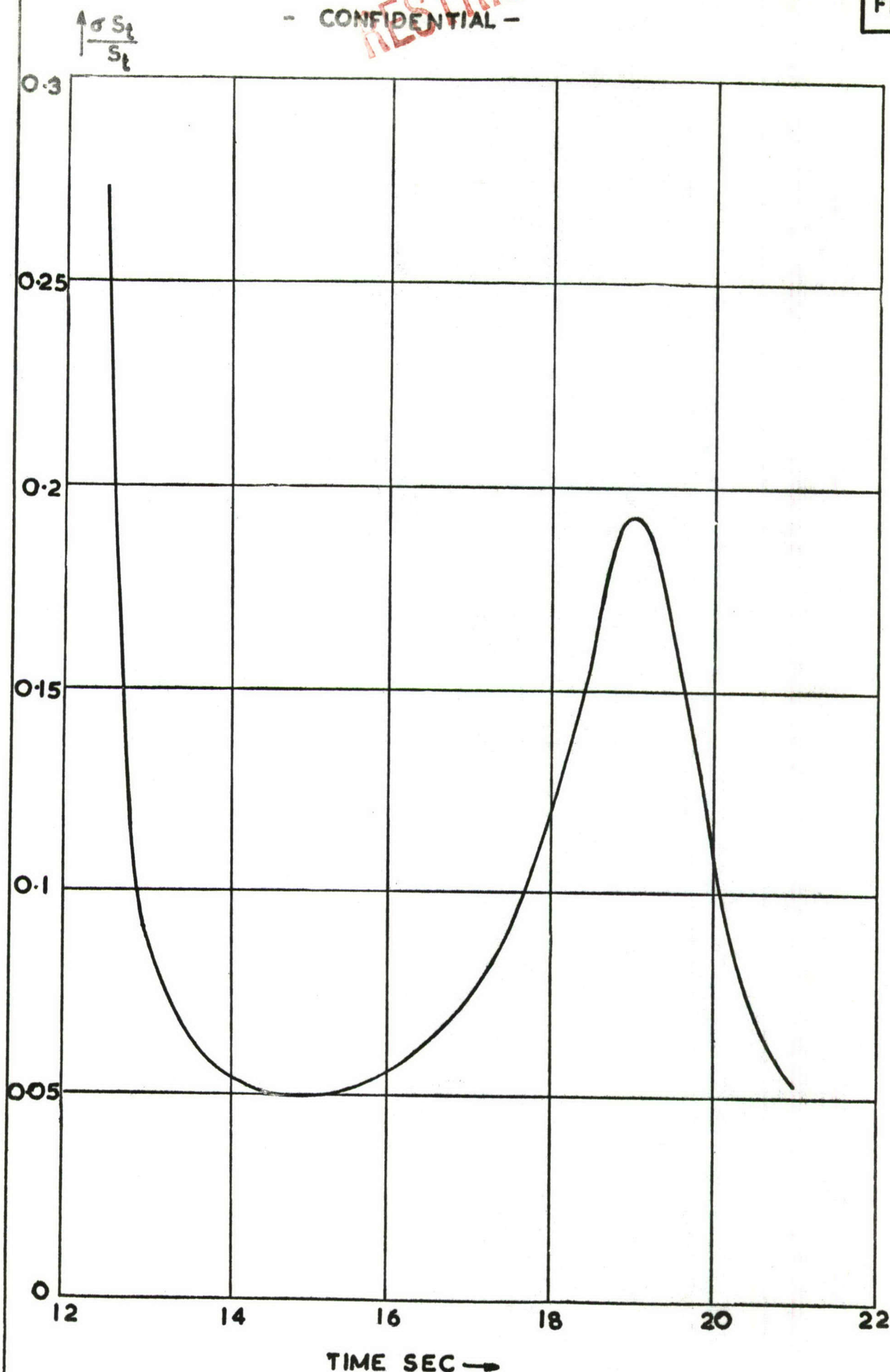

FIG 3. TYPICAL ERRORS IN EXPERIMENTAL STANTON NUMBER VS. FLIGHT TIME FOR DATA OF REFERENCE 5.

FIG.4.

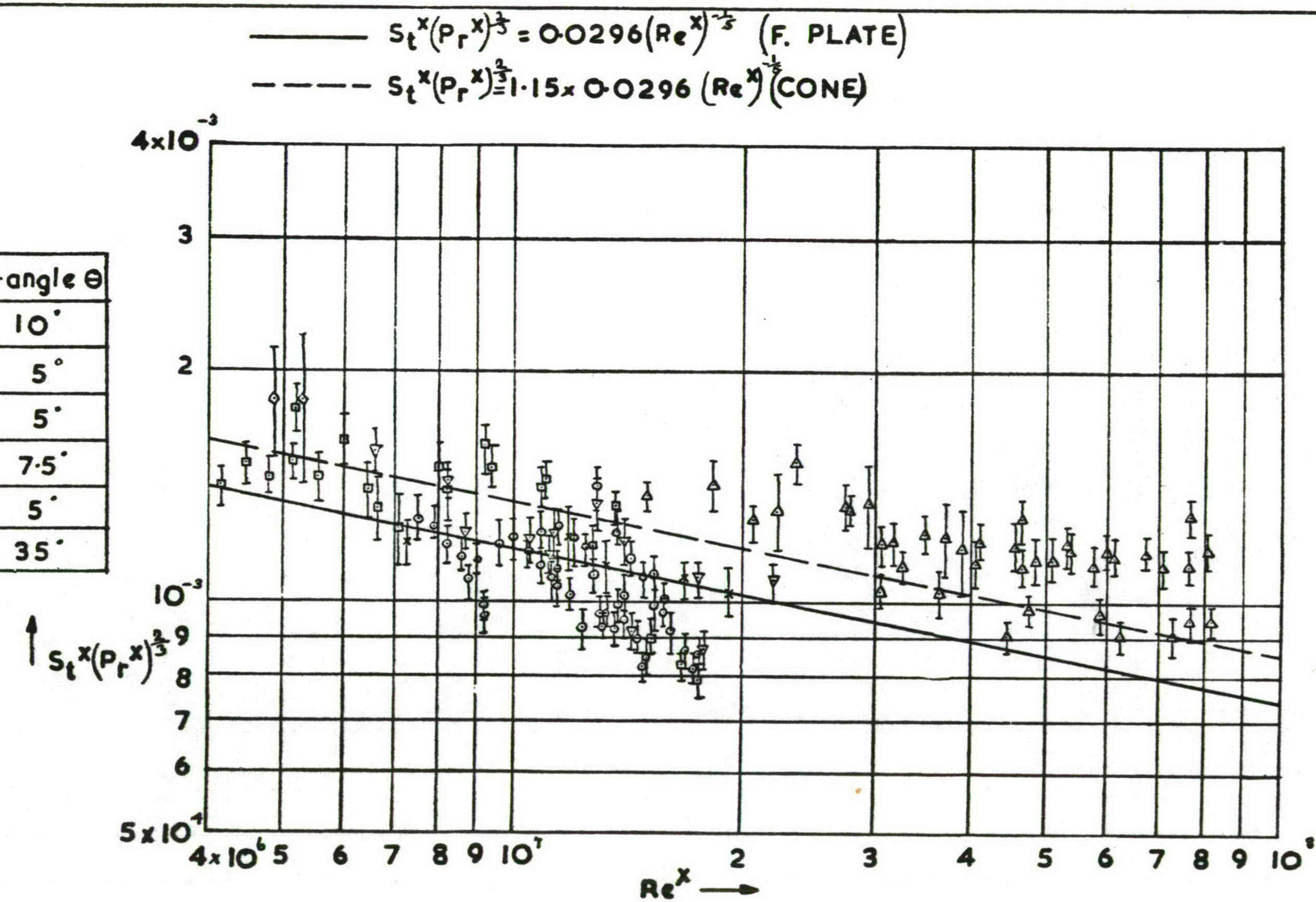

REF.	symbol	½-angle θ
1	⊙	10°
2	×	5°
3	△	5°
4	⊡	7·5°
5	▽	5°
6	◇	35°

FIG.4. VARIATION OF $S_t^x (P_r^x)^{\frac{2}{3}}$ WITH R_e^x FOR POINTS HAVING ERRORS IN $S_t^x \leq 10\%$

(P.1167).

FIG.5.

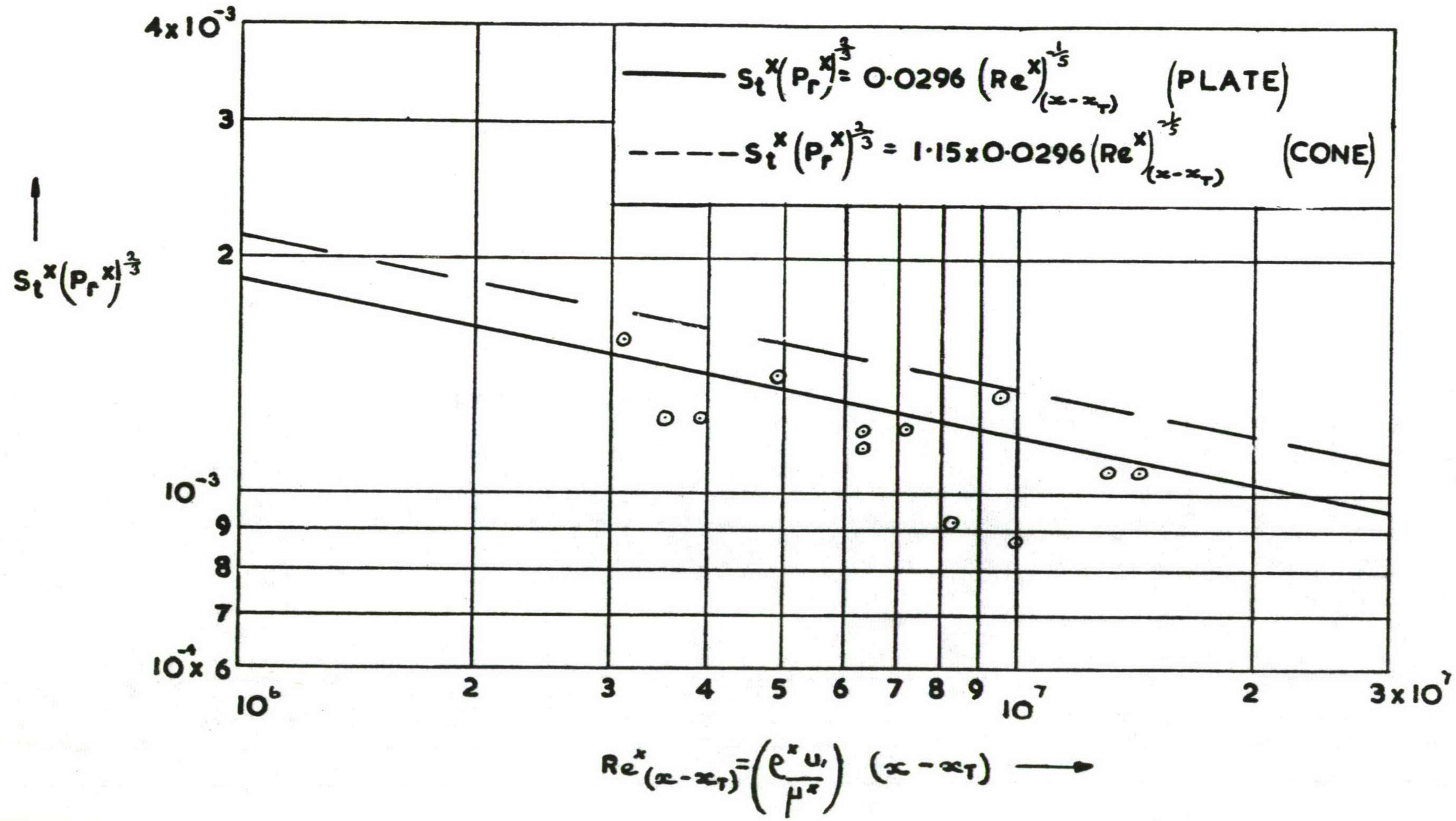

FIG.5. VARIATION OF $S_t^x (P_r^x)^{\frac{2}{3}}$ WITH $Re^x_{(x-x_T)}$ FOR RESULTS ON $5^\circ \frac{1}{2}$-ANGLE CONE. (REF. 5).

(W.1167).

FIG.6.

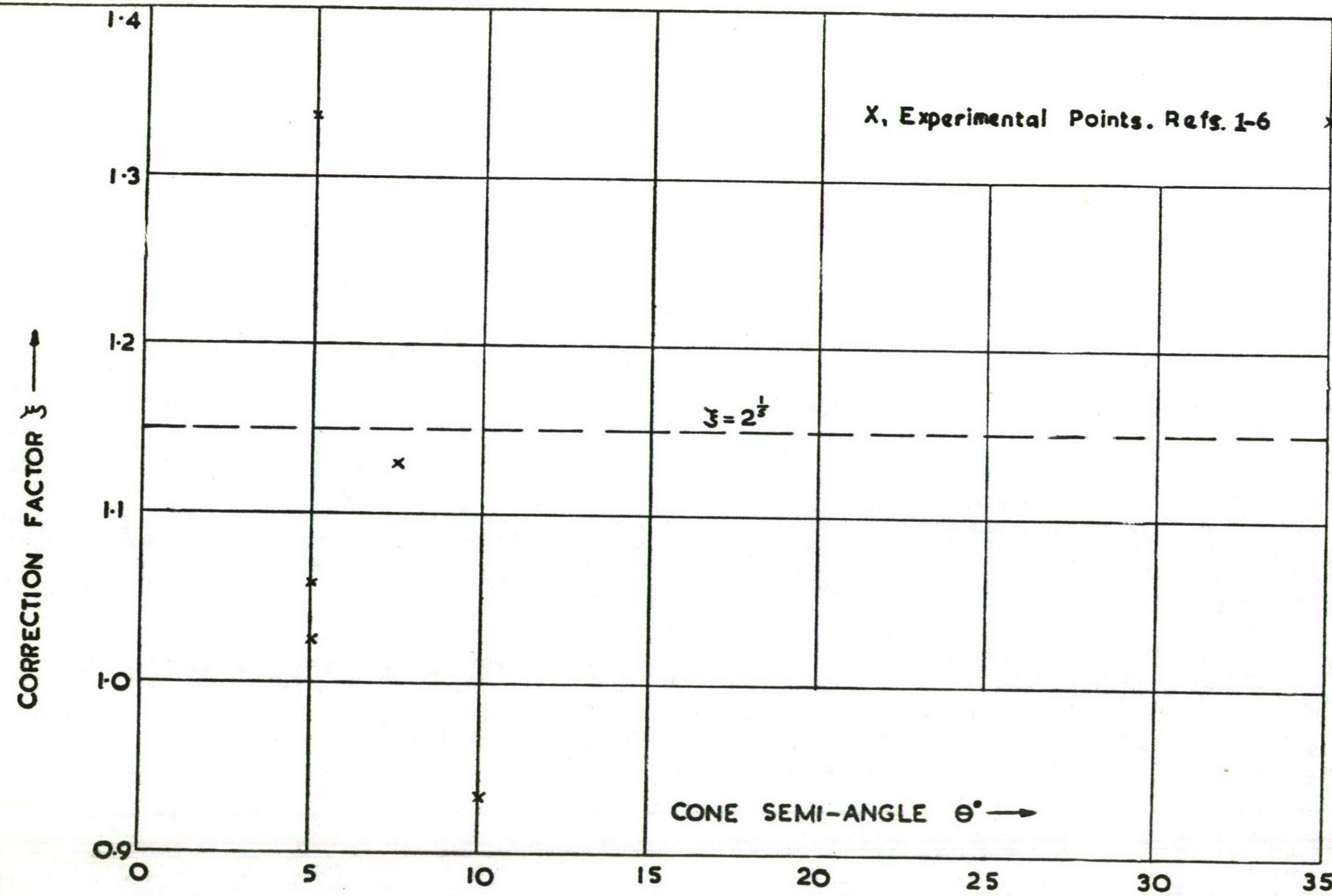

FIG 6 VARIATION OF CORRECTION FACTOR ζ OBTAINED FROM EQUATION (1.) WITH CONE SEMI-ANGLE θ

(MR.1167).

FIG. 7.

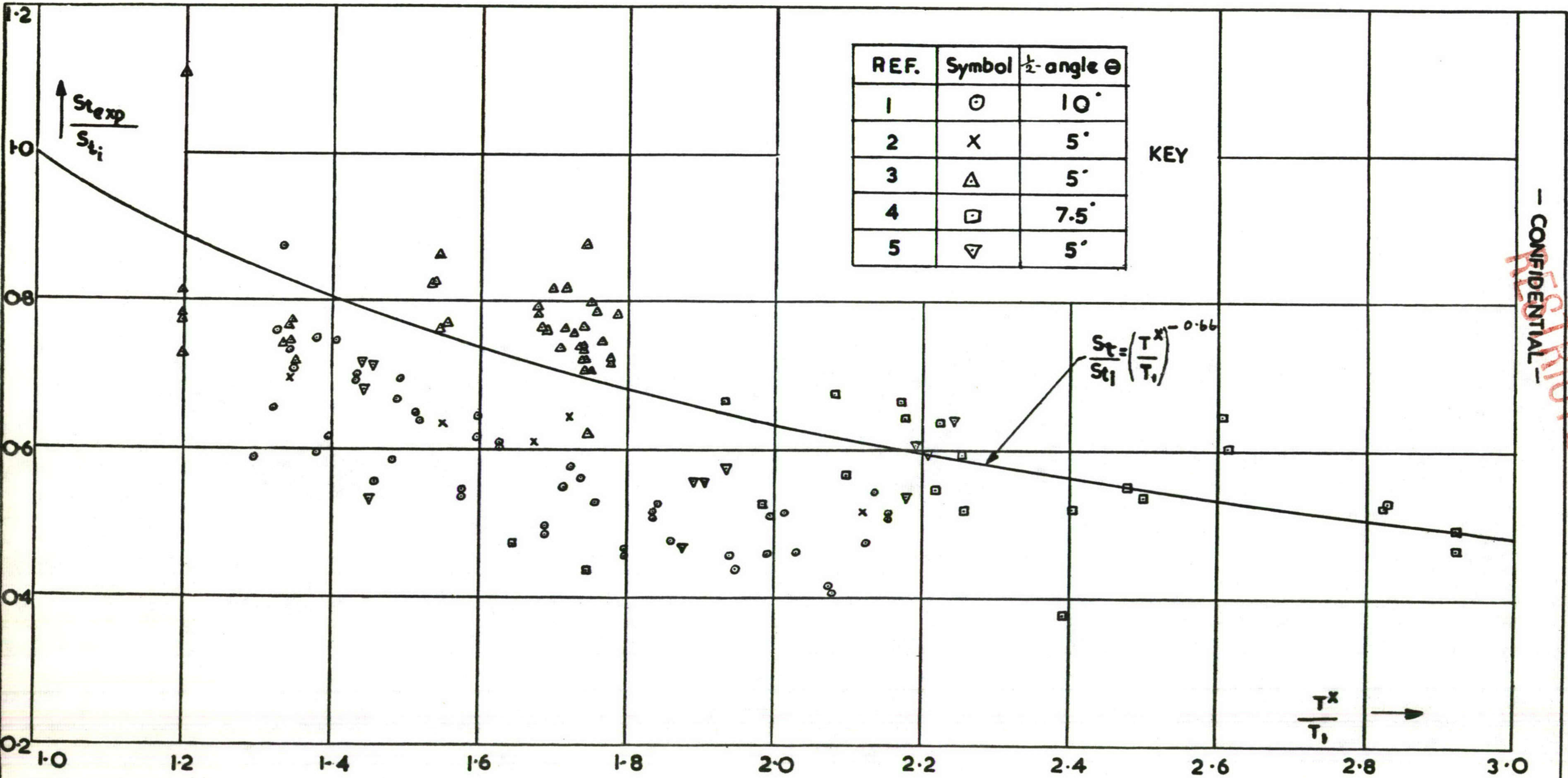

REF.	Symbol	½-angle θ
1	⊙	10°
2	×	5°
3	△	5°
4	⊡	7.5°
5	▽	5°

FIG. 7. CORRELATION OF EXPERIMENTAL TO THEORETICAL INCOMPRESSIBLE STANTON N°. RATIO WITH INTERMEDIATE TEMPERATURE RATIO.

(W.1167)

T_w/T_1	Symbol
1·0-1·5	×
1·5-2·0	⊙
2·0-2·5	△
2·5-3·0	⊡
3·0-3·5	▽

THEORETICAL LINES SHOWN ARE BASED ON EQN. (8) OF APPENDIX II.

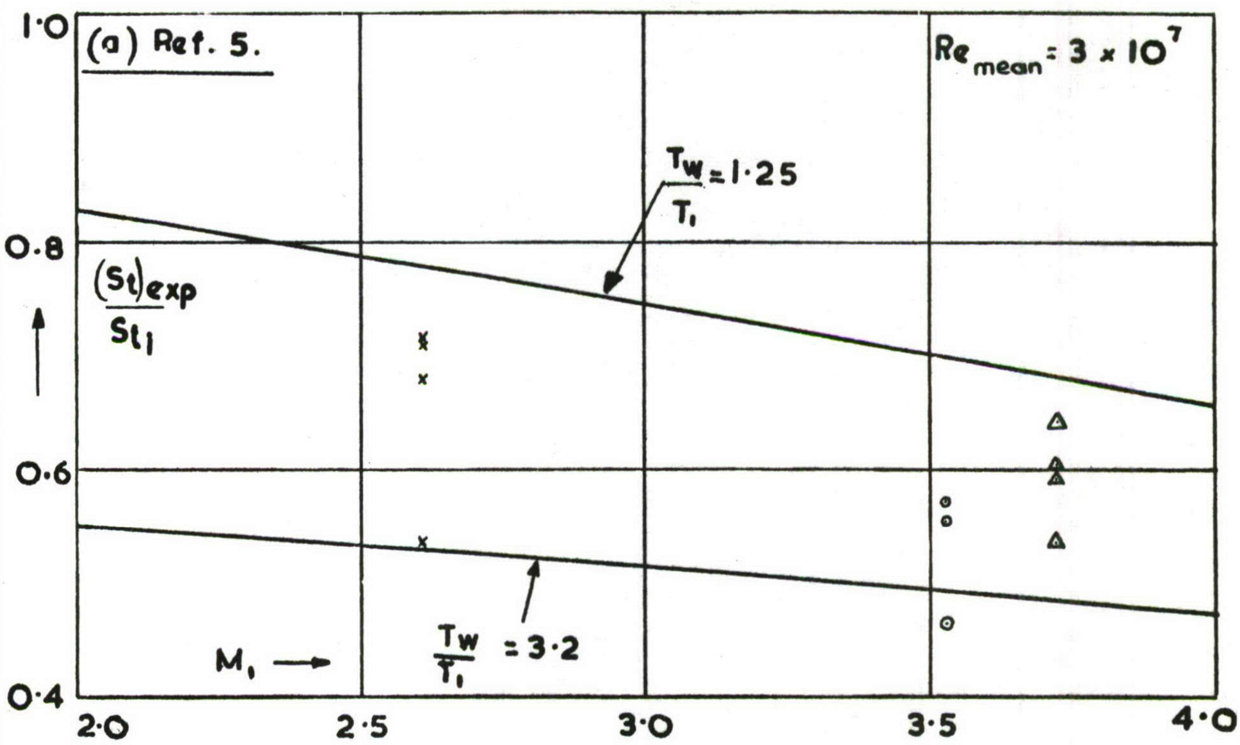

FIG.8. (a to e) VARIATION OF $\{(St)_{exp}/St_i\}$ WITH LOCAL MACH NUMBER AND WALL TEMPERATURE RATIO (T_w/T_1).

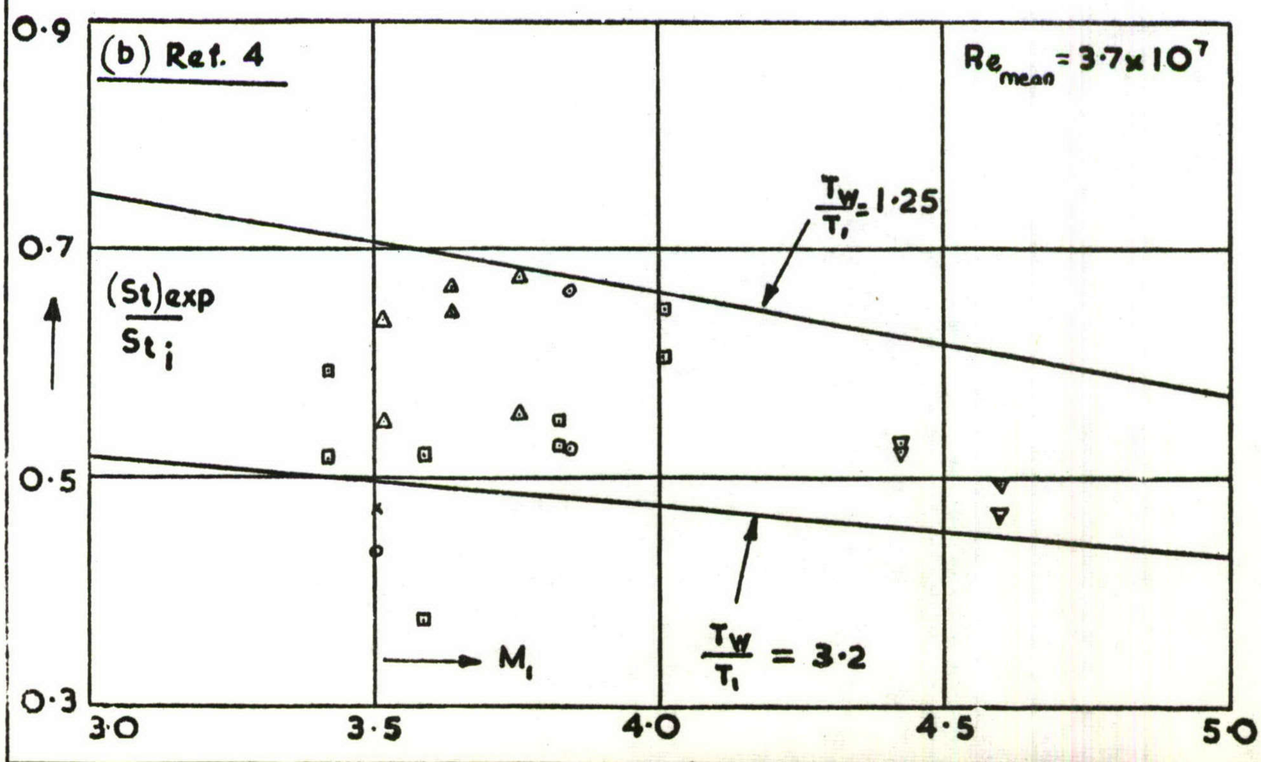

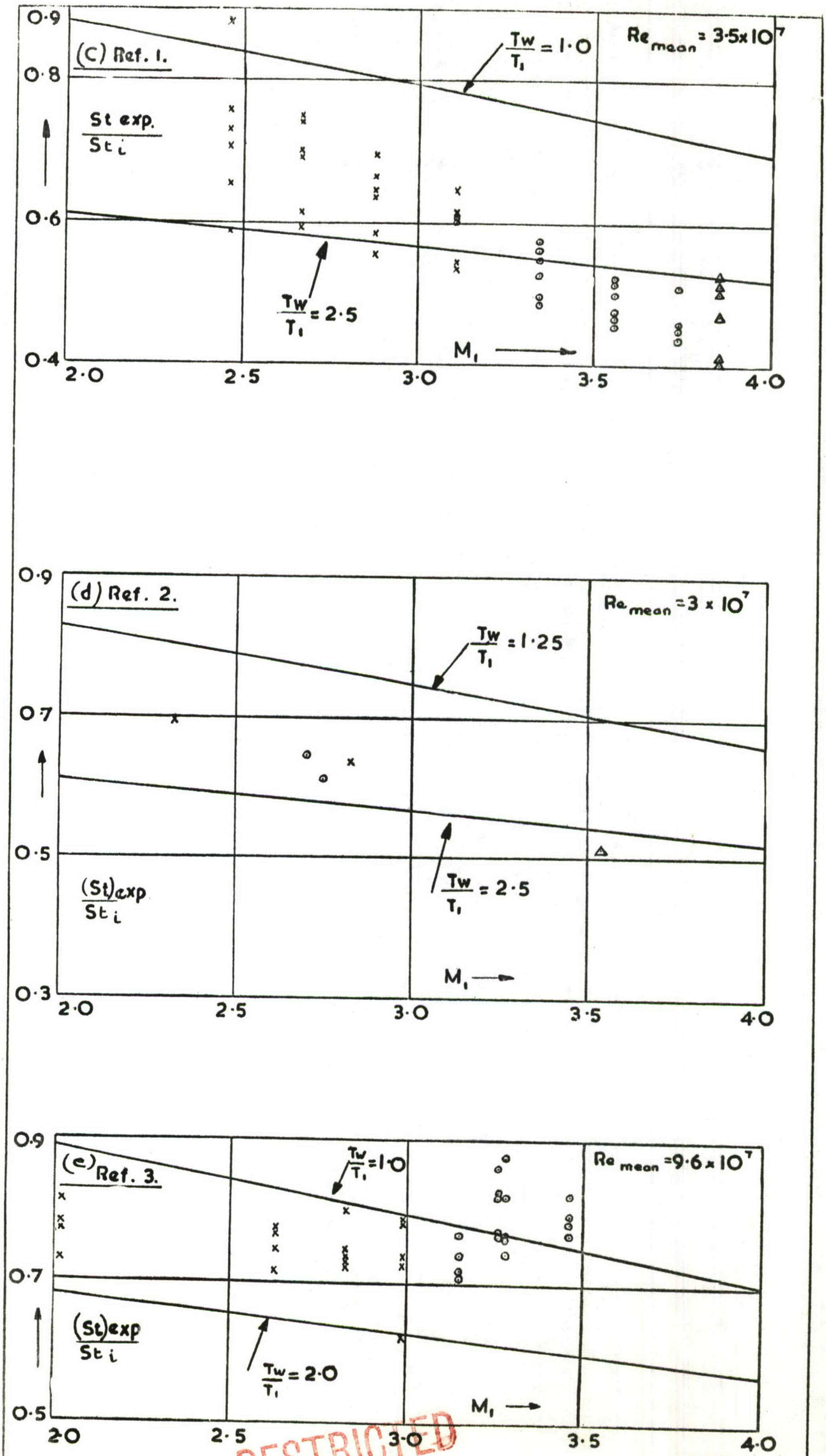

RESTRICTED

CONFIDENTIAL

FIG 8c-e

KEY (FIGS. 9 & 10).

REF.	Symbol	½-angle θ
1	⊙	10°
2	×	5°
3	△	5°
4	⊡	7.5°
5	▽	5°
6	◊	35°

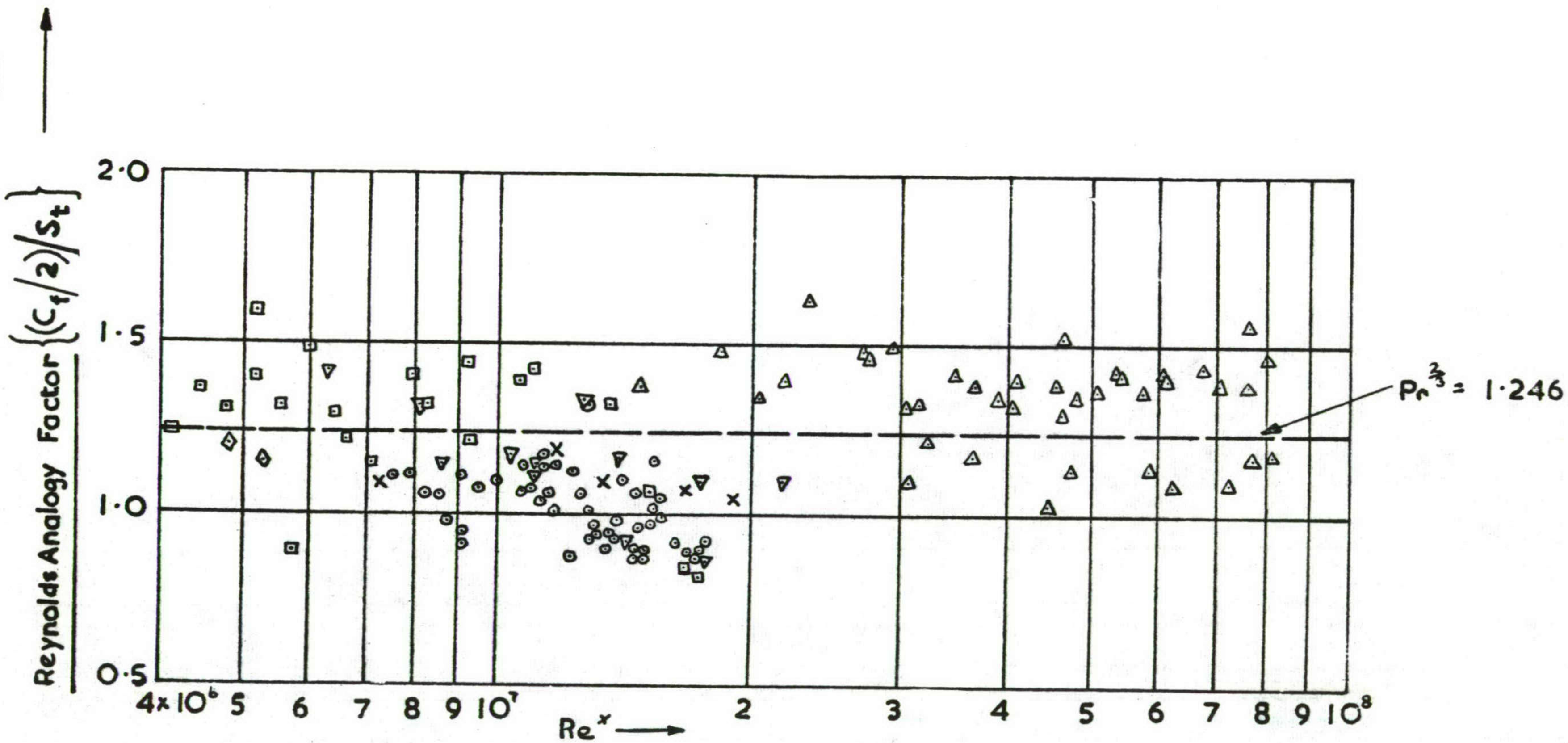

FIG. 9. VARIATION OF REYNOLDS ANALOGY FACTOR $\{(C_f/2)/S_t\}$ WITH Re^x.

(WP.1157).

KEY SEE FIG.9

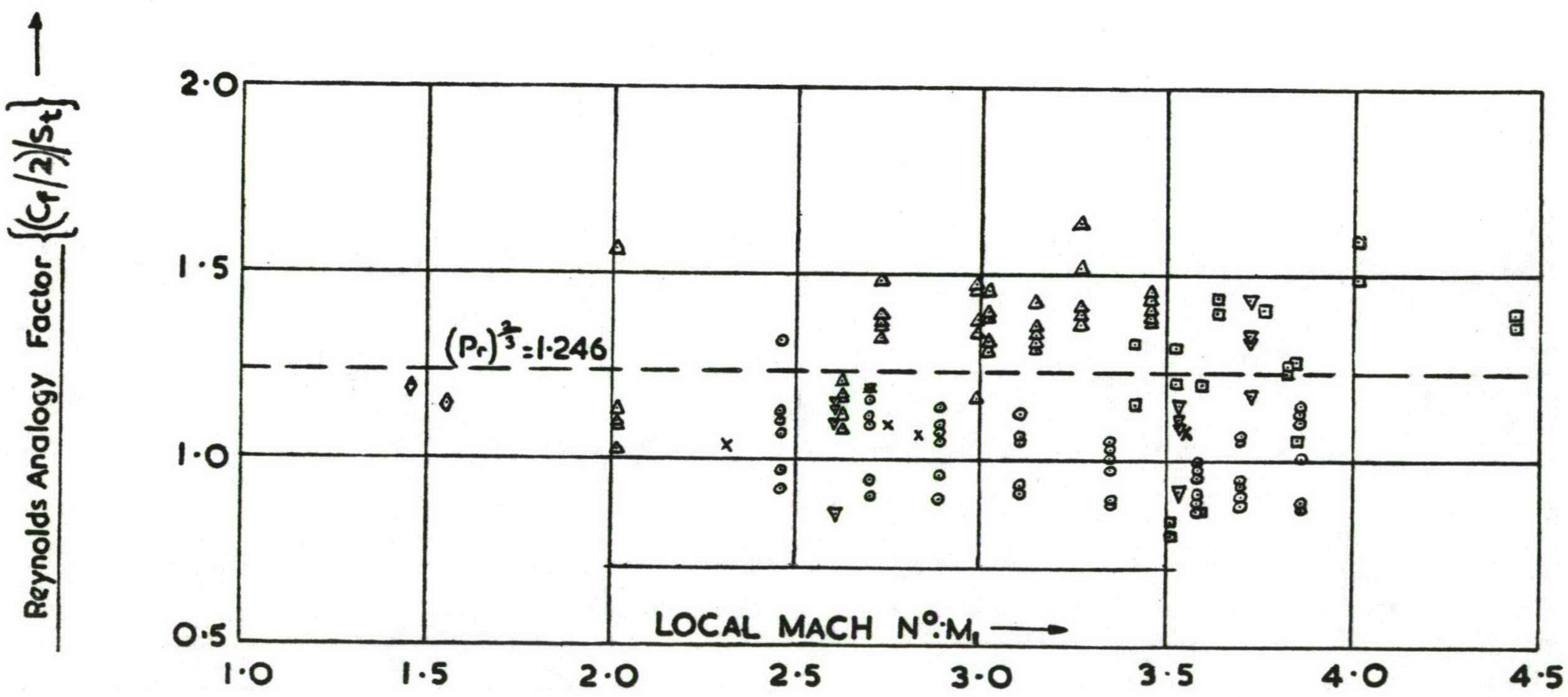

FIG. 10. VARIATION OF REYNOLDS ANALOGY FACTOR $\{(C_f/2)/S_t\}$ WITH LOCAL MACH NUMBER M_1.

(MP.1167).

+ Experimental Points Refs:– 2, 3, 6 & 7

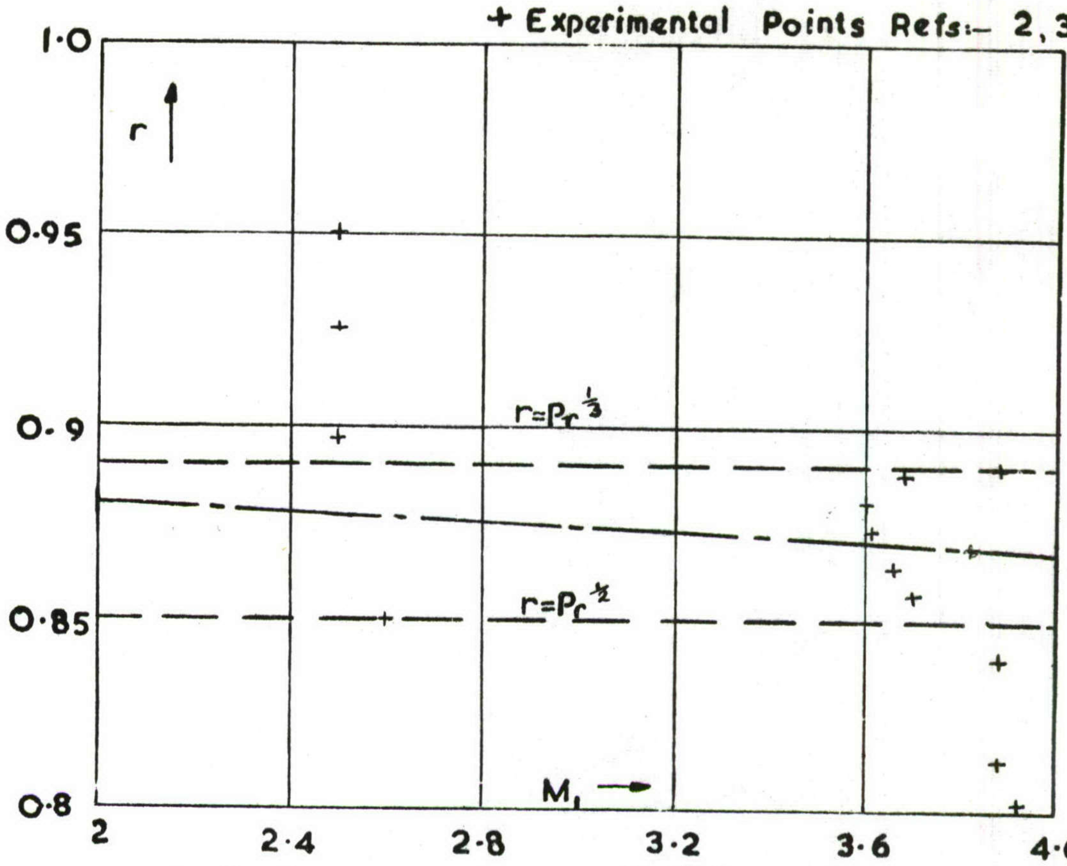

———— Tucker & Maslen For $u/u_1 = (y/\delta)^{1/7}$ (Ref. 8.)

FIG. 11. VARIATION OF TURBULENT FLOW TEMPERATURE RECOVERY FACTOR WITH LOCAL MACH NUMBER.

FIG 12. VARIATION OF TURBULENT FLOW TEMPERATURE RECOVERY FACTOR WITH LOCAL REYNOLDS NUMBER.

⊙ Experimental Points. Refs. 2, 3, 6 & 7.

– – – Extrapolation From Data For Continuous Flow Tunnels (Ref. 9.)

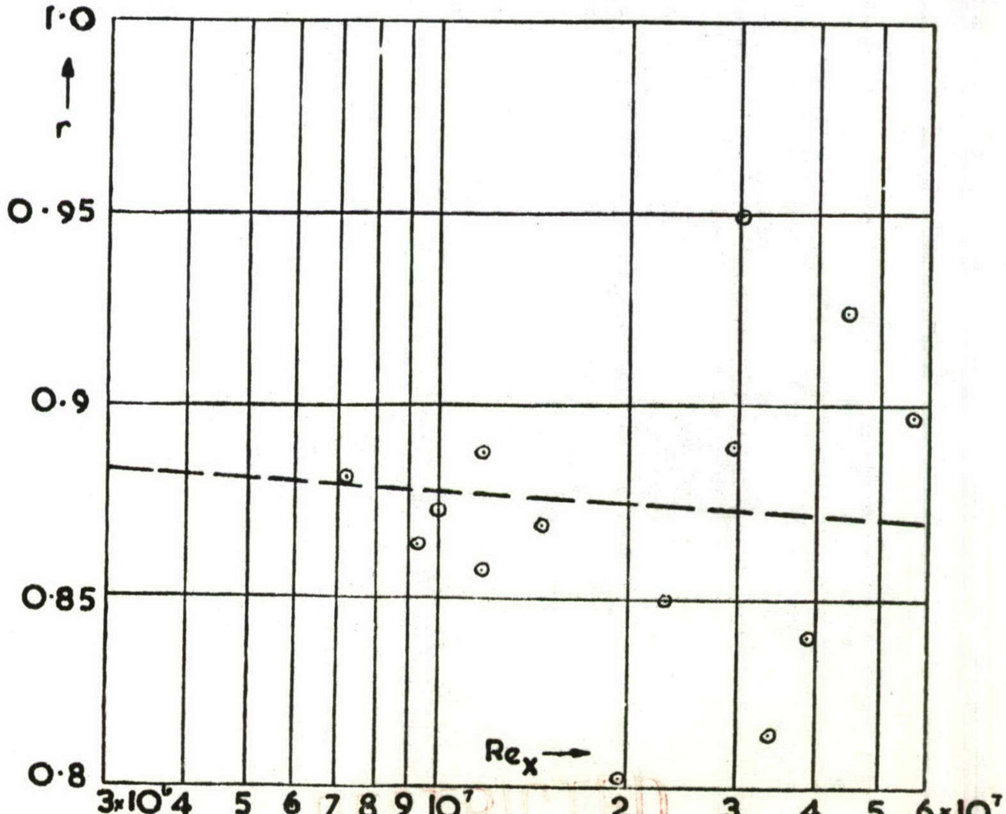

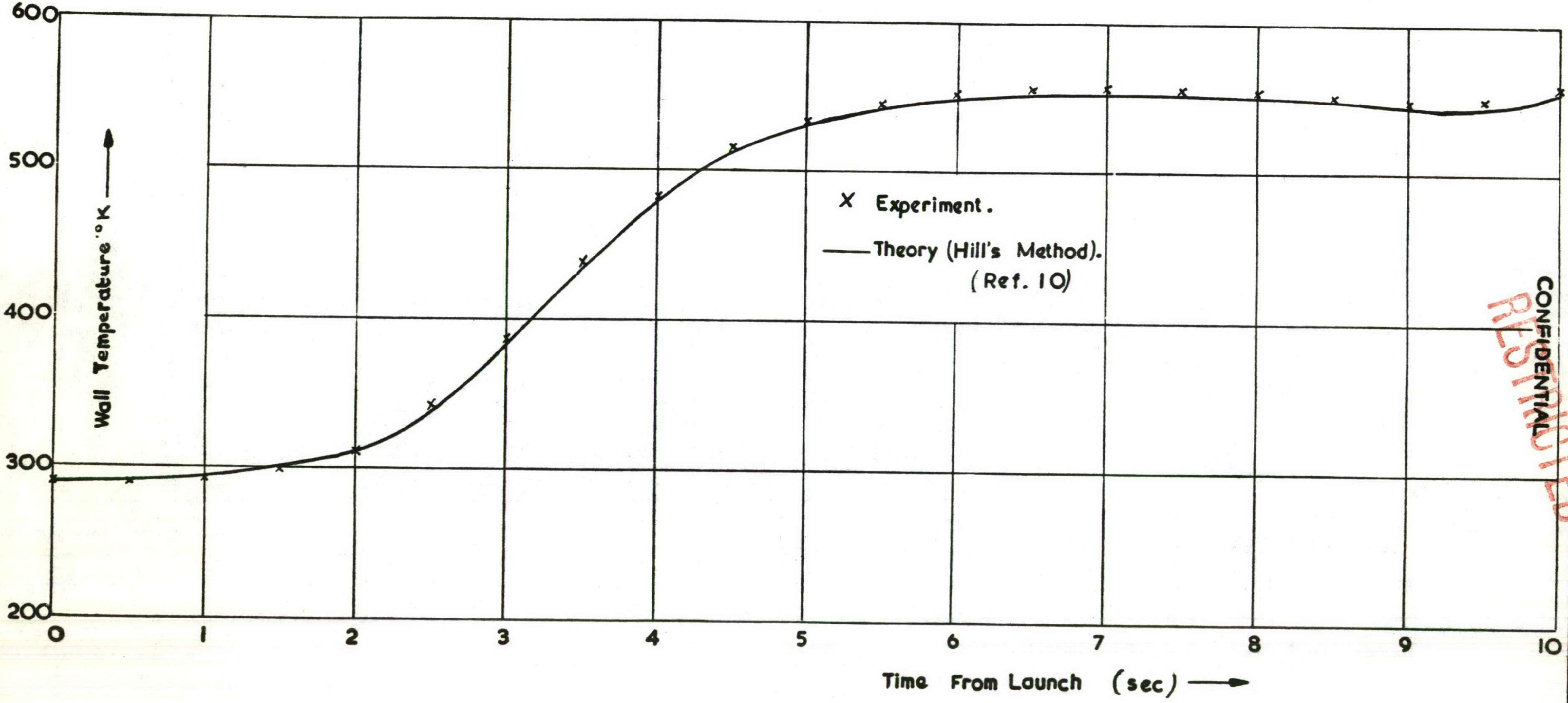

FIG. 13. VARIATION OF WALL TEMPERATURE WITH TIME AT STATION 22·5" FOR 5° CONE (REF. 2).

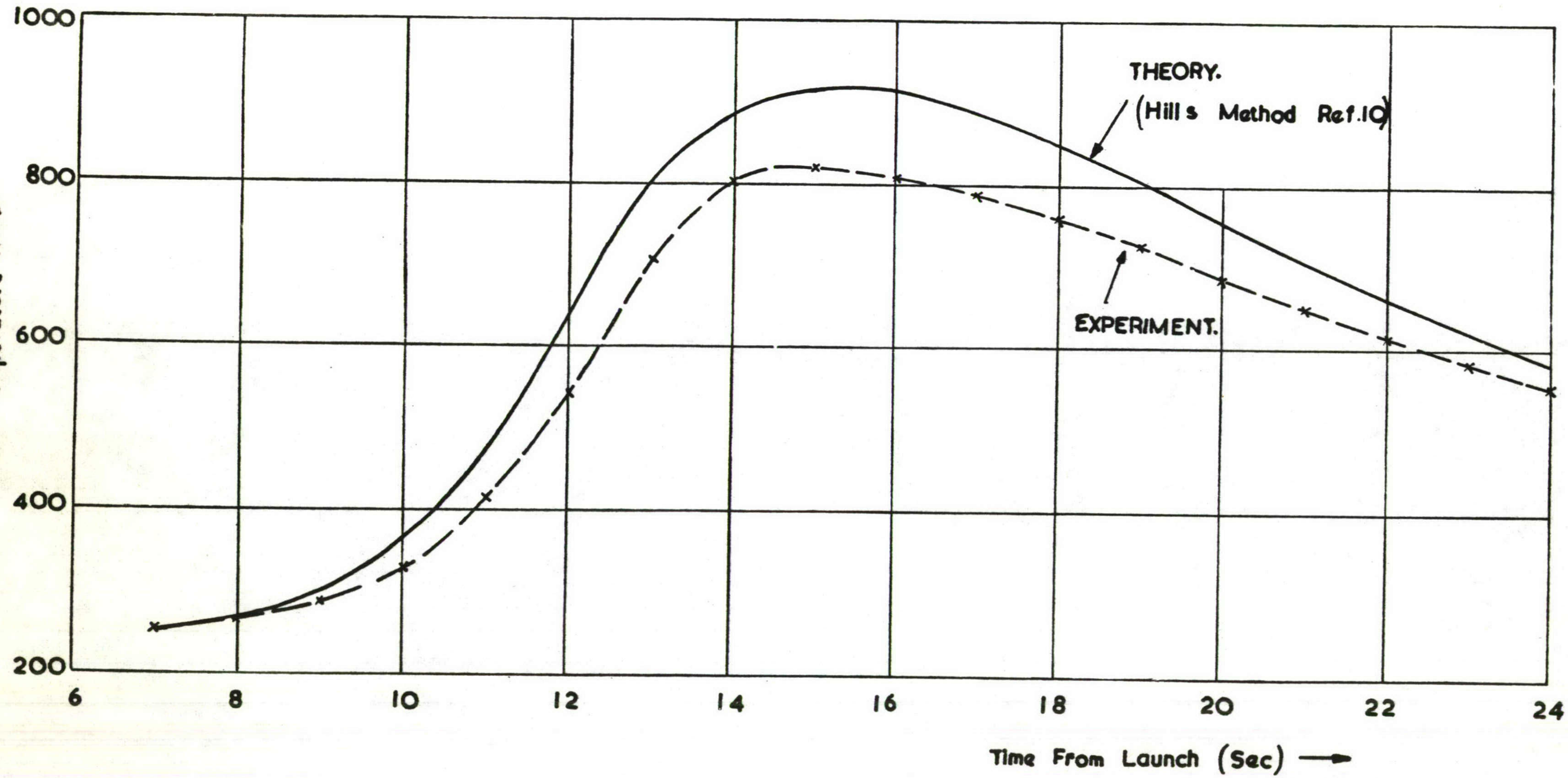

FIG. 14. VARIATION OF WALL TEMPERATURE WITH TIME AT STATION 11·66" FOR 35° CONE (REF. 6).

US ARMY STANDARDIZATION GROUP, UK
Box 65, USN 100, F.P.O.
New York, N.Y.

ORD-AE-J-3030-20 — 21 January 1964

SUBJECT: Transmittal Document

TO: See Distribution

Forwarded herewith for information and retention is British Aircraft Corporation Limited (GW Div.) Technical Report No.75, entitled, "A Correlation of Free Flight Aerodynamic Heat Transfer Measurements on Pointed Cones", dated January, 1962.

FOR THE SENIOR REPRESENTATIVE:

1-Incl:
a/s

WILLIAM A. DAUGHERTY
Lt Colonel, Sig.C.
GM/Elect.Representat ve

Distribution:
w/Incl: AMSMI
AMCPT-TP-TD
AMXBR
CG WSMR
CO Picatinny Asnl
w/o Incl: ArmA London

If Inclosure is withdrawn the classification of this document will be down raded to UNCLASSIFIED

Reg # 59811

[dstl]

Information Centre
Knowledge Services
[dstl] *Porton Down,*
Salisbury
Wilts
SP4 0JQ
22060-6218
Tel: 01980-613753
Fax 01980-613970

Defense Technical Information Center (DTIC)
8725 John J. Kingman Road, Suit 0944
Fort Belvoir, VA 22060-6218
U.S.A.

AD#: AD345966

Date of Search: 22 July 2008

Record Summary: DSIR 23/29382
Title: A Correlation of Free Flight Aerodynamic Heat Transfer Measurements on Pointed Cones (Bristol Aircraft Ltd, GW Engineering Dept TR 75
Availability Open Document, Open Description, Normal Closure before FOI Act: 30 years
Former reference (Department) ARC 23545
Held by The National Archives, Kew

This document is now available at the National Archives, Kew, Surrey, United Kingdom.

DTIC has checked the National Archives Catalogue website (http://www.nationalarchives.gov.uk) and found the document is available and releasable to the public.

Access to UK public records is governed by statute, namely the Public Records Act, 1958, and the Public Records Act, 1967.
The document has been released under the 30 year rule.
(The vast majority of records selected for permanent preservation are made available to the public when they are 30 years old. This is commonly referred to as the 30 year rule and was established by the Public Records Act of 1967).

This document may be treated as UNLIMITED.